R. & M. No. 2253
(9892)
A.R.C. Technical Report

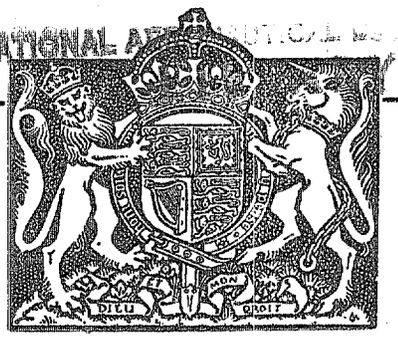

MINISTRY OF SUPPLY

AERONAUTICAL RESEARCH COUNCIL
REPORTS AND MEMORANDA

Measurements of the Degree of Smoothness Attained in a Laminar-Flow Wing Specimen (Short Bros.)

By

R. B. Coles, B.Sc. (Eng.)

LONDON : HIS MAJESTY'S STATIONERY OFFICE

1949

Price 4*s*. 6*d*. net

Measurements of the Degree of Smoothness Attained in a Laminar-Flow Wing Specimen (Short Bros.)

By

R. B. Coles, B.Sc. (Eng.)

Communicated by the Principal Director of Scientific Research (Air), Ministry of Supply

Reports and Memoranda No. 2253

May, 1946*

Summary.—This report describes tests made to determine the degree of surface smoothness attained in a 6-ft. chord wing specimen having two spars and a thin skin stiffened between spars by ribs and channel section chordwise members. The specimen was designed and made by Short Bros. of Rochester.

The tests included measurements of the initial surface smoothness, distortion under load, proof and ultimate tests and compression tests on two short lengths of the upper front spar flange. These tests show that in order to reduce the amplitude of the skin distortions to the required limits the rigidity of the channel section stiffeners should be increased and possibly additional local stiffening near the front spar added. No permanent distortions of the wing beyond the allowed limits are likely to occur under service conditions.

The compressive stress in the spar flanges at failure was 37,500 lb./sq. inch. Strut tests on 6-in. and 12-in. lengths of the upper front spar flange gave failing stresses of 59,000 lb./sq. in. and 48,000 lb./sq. in. respectively.

LIST OF ILLUSTRATIONS

*R.A.E. Report. No. S.M.E. 3374 received 16th August, 1946.

1. *Introduction.*—The development of laminar-flow wing sections involves making a wing with a high degree of smoothness from the leading edge to about half the chord. A wing of this type must remain smooth when subjected to loads arising from mild manoeuvres while the aircraft is flying at its maximum or cruising speed and must not develop permanent distortions during severe manoeuvres.

An extensive test programme to investigate the suitability of various types of construction has been in progress.

The first specimen tested by King[1] (1945), was of box construction using a heavy gauge skin reinforced by spanwise corrugations. The present report describes the work on the second specimen, a two spar type with a light skin and chordwise stiffening only. This second specimen in contrast to the first, has its strength and stiffness in the spars rather than in the skin. The distortions under load of these two wing surfaces are somewhat different, the first type of construction develops small distortions of short wavelength occurring between crests of corrugations, the second has larger distortions but much longer wavelength. This may be an advantage since the criterion for surface waviness is the ratio of wave depth to wavelength and it may be less critical for long wavelength distortions.

The specimen tested was a 6-ft. chord uniform section wing made by Messrs. Short Bros. and representing the construction of the Sturgeon wing. The specimen had been previously tested for its aerodynamic qualities in the wind tunnel at the National Physical Laboratory and reported by Richards, Walker and Thwaites[2] (1945).

2. *Results of Investigation.*—2.1. *Initial Smoothness.*—Measurements of the rivet head smoothness (Fig. 6) show that the majority are very near the required smoothness limits. Rivet numbers 1, 2, 10, 14 and 21 are considered to be sufficiently smooth and rivets 5, 6, 7 and 22 too rough. The chief fault being that the rivet edge " step " is too high, however, some rivets such as 12, 24 and 27 have a rough head, probably caused by a letter " S " stamped on each rivet head. The riveting caused little dimpling of the sheet.

Measurements of the skin joint " step " (Fig. 6) show that the height of the " step " varied considerably from values which are within the smoothness limit, such as sections P, R and E, to values approximately four times the permissible.

The chordwise waviness measurements show that on both surfaces the waviness is more serious near rivet lines indicating that the riveting causes some disturbance to the smoothness. On both surfaces the waviness is more pronounced where the curvature is small. Fig. 9 shows the lengths on the various measuring sections where the waviness exceeds the limit of smoothness *i.e.* $\frac{\text{Wave height}}{\text{Wave length}} = \frac{1}{1000}$. This smoothness limit is probably too large, recent work indicates that this limit should be $\frac{1}{2000}$; however, for purposes of this report the $\frac{1}{1000}$ ratio will be used.

2.2. *Distortion under Load.*—The surface distortions caused by loads corresponding to maximum level speed conditions are shown in Figs. 10–14. The magnitudes of these distortions are somewhat large but owing to their long wavelength are not as critical as it would appear. The height/wavelength ratios for these distortions are shown in Fig. 14.

The most serious distortion is the concave wave formed over the front spar. The magnitude of this wave would be considerably reduced by local stiffening near the spar.

Spanwise plots of the skin distortion (Fig. 13) show that the channel section chordwise stiffener has very little value in reducing the dimensions of the skin distortions. The behaviour under load of this specimen would be considerably improved if full sheet web ribs were used in place of the channel section stiffeners.

As was found in the case of the Armstrong Whitworth specimen, surface distortions under level flight conditions are mainly caused by the aerodynamic suction, represented in these tests by internal air pressure, A further point of interest is that although the surface of the wing is appreciably distorted under level flight conditions, the skin still retains its initial waviness. This is shown by the measurements taken over section D shown in Fig. 13.

Proof tests to find at what load permanent distortion of the wing occurred were made under case A loading conditions up to a factor of $n = 10$ (approx. 8,500 lb./sq. in. in upper spar flanges).

No permanent distortion of the specimen was measured. During these tests slight buckling of some panels was noticed at a factor of $n = 3$ (stress in upper spar flanges 1,600 lb./sq. in.) at $n = 5$ (2,700 lb./sq. in.) buckling of the whole surface was observed. The estimated buckling stress for the top surface is 2,200 lb./sq. in. corresponding to a factor of $n = 4 \cdot 1$ under these loading conditions.

The internal air pressure was not increased with factor above its value at $n = 6$, this caused the sudden change of slope on the load deflection curves for the skin distortions. The air pressure was not increased above this value as the ultimate factor for these loading conditions was $7 \cdot 5g$ and the pressure is a function of the speed and not the stress conditions in the structure.

There was no permanent distortion of the specimen under aileron case C loads up to the ultimate factor for this case of $n = 2$. The shear stresses at $n = 2$ were 2,000 lb./sq. in. and 2,600 lb./sq. in. in the nose and inter-spar shells respectively.

2.3. *Ultimate Strength.*—The specimen was tested to destruction under case A loads, failure occurred at a factor of $n = 21 \cdot 15$, a photograph of the failure is shown in Fig. 19. The failing stress in the upper spar flanges was 37,500 lb./sq. in. This value is considerably lower than the failing stress of the spar flange when tested as a strut (48,000 lb./sq. in. and 59,000 lb./sq. in. for 12-in. and 6-in. lengths respectively). The calculated instability stress for the spar flange when the compressive stresses are uniformly distributed over the width of the sides of the angle, is 35,000 lb./sq. in. which is in agreement with the failing stress of the spar in the ultimate strength test. The torsional instability stress for this flange was found to be 34,000 lb./sq. in. The higher values of failing stress obtained from the strut tests are probably due to the difference in end constraints in the two cases.

PART II

Description of Specimen and Experimental Investigation

3. *Description of Specimen.*—The specimen represented the wing construction of the Short Sturgeon at a point 3 ft. $10\frac{1}{2}$ in. from the wing tips where the chord is 6 ft. It comprised an 8 ft. 10 in. length having a constant chord of 6 ft. and an NACA 64–2–(25)15 aerofoil section adapted for a thickness-chord ratio of 15·6 per cent. and a camber of $a = 0 \cdot 4$. The maximum thickness of this section occurs at 40 per cent. chord. For the structural tests only that part of the specimen forward of the rear spar was used. The rear spar compression flange was located at approximately 60 per cent. chord and the behaviour under load of the wing aft of this point is of minor interest since it is beyond the region of laminar flow.

The weight of the specimen including the trailing edge was 13 lb. per ft. spanwise.

3.1. *Type of Construction.*—A cross-section of the specimen including the trailing edge and details of the construction is shown in Fig. 1. The 18-gauge dural spar webs were inclined to facilitate wing folding. The spar upper flanges of extruded angle sections (D.T.D. 364A) were

situated at approximately 20 per cent. and 60 per cent. of the chord. Nose and inter-spar ribs were 22-gauge D.T.D. 390 dural, the nose ribs being spaced 6 in. apart and the inter-spar ribs 12 in. The wing surface between the inter-spar ribs was further stiffened by a channel section member of 18-gauge dural midway between adjacent inter-spar ribs. The skin was 18-gauge D.T.D. 390 dural. Spanwise skin joints were made over the spar flanges. An additional butt skin joint on the lower surface at 37·5 per cent. chord was made necessary by the method of construction described in section 3.2.

3.2. *Method of Manufacture.*—The nose sheeting, which was continuous from the upper to the lower front spar flanges, was stretch pressed until it exactly fitted a nose profile jig, consisting of a number of thick bakelised-fabric female nose formers. The nose ribs, having been previously aligned by telescope and collimator, were held in position by a suitable jig while the nose sheeting was attached. The nose was assembled by spigot bolts to the front spar and the nose sheeting riveted to the top and bottom spar flanges. The complete nose unit, inter-spar stiffeners and rear spar were then erected in an assembly jig and the top and bottom skins riveted up. Access for this riveting was provided by an under-surface panel (Fig. 1) which was finally closed with " pop " rivets.

All external riveting was carried out by reaction methods. No special equipment or method of riveting was used other than taking particular care in the selection of rivets and careful supervision during manufacture.

No special technique was used in making the skin joints. The tops of the spar flanges were preshaped to the appropriate aerofoil section and the skin attached by a single row of rivets ; no packing was used to align the sheets more satisfactorily. The sheets used for the specimen were carefully selected to be as far as possible free from initial waviness.

3.3. *End Reinforcements.*—After completion of the wind tunnel tests the ends of the specimen were reinforced for attachment of the loading rig. The method of reinforcing the ends, which was to attach diffuser plates to the wing skin and spars is shown in Fig. 2. Steel end bulkheads ($\frac{5}{8}$-in. thick) were attached to the ends of the specimen by a stiffened angle section made to the wing profile. These end bulkheads served the double purpose of sealing the ends of the specimen and applying the torsion and bending loads. Suitable connections were provided for the air pressure supply and measuring lines.

4. *Range of Investigation.*—Measurements of the surface smoothness of the specimen were made before any loads were applied. Following these initial measurements a series of tests were made to investigate the behaviour of the end bulkheads under load. From these tests it was hoped to determine to what extent the end bulkheads remained plane under load and to find the location of the loading point, in a fore-and-aft direction, which would ensure that the bending moment caused uniform angular strain at all points along the chord. The bending load was applied in turn to each of three loading points, which were spaced 3 in. apart in a fore-and-aft direction. The angular rotation of the end bulkheads about a horizontal axis indicated that they were sufficiently stiff to remain plane under load. A comparison between the angular rotation about a vertical axis for each position of the point of load application indicated that either the central or forward loading position should be used to give uniform angular strain across the chord. It was decided to use the forward position and subsequent tests in which bending deflections of the spars were measured showed that this position caused equal deflections of the spars.

The three major tests detailed below were then made.

(1) Elastic distortion tests to determine the amount of distortion of the wing surface likely to occur in flight under a normal acceleration of $1\frac{1}{4}g$.

(2) Proof tests to determine the load required to produce permanent distortion of the wing surface beyond the allowable limits.

(3) A final test to determine the failing load of the specimen. After the completion of these tests, strut tests and torsional stiffness tests were made on a length of spar flange of the same section and material as the upper front spar flange of the specimen.

5. Loading Conditions.—The loads applied to the specimen were those appropriate to the wing section used.

The method of loading prevented the correct stress distribution between the top and bottom surfaces being obtained. The bending load was adjusted to make the top surface conditions, at any given factor, representative, as this surface is more critically loaded as far as skin distortion are concerned. No attempt was made to represent vertical shear loads in any of the tests.

The method of testing smooth wing specimens has been fully described by King and Trollope[3] (1945).

The test loads and the corresponding flight cases are detailed below.

5.1. *Elastic Distortion Tests.*—The test loads represented a normal acceleration of $1\frac{1}{4}g$. occurring at the maximum level speed of 330 m.p.h. E.A.S. The test case is shown on the rationalised stressing diagram in Fig. 3 together with the test loads. The chordwise pressure distribution at factors $1g$ and $1\frac{1}{4}g$ are shown in Fig. 4 the test pressure being marked for comparison.

5.2. *Proof Tests.*—For this series of tests, loads corresponding to case A and a modified case C were used. Case A loading was chosen since this gives a low value to the internal air pressure and as the internal pressure has a stabilising effect on the skin buckling, this is an adverse case from the buckling point of view. Since aileron case C loading produces the highest torques, it was chosen to ascertain the effect of shear on the skin buckling. The two cases are marked on the rationalised stressing diagram (Fig. 3). The corresponding test loads at unity factor are shown tabulated in the same figure.

The chordwise pressure distributions for these two flight cases are shown in Fig. 4.

5.3. *Ultimate Strength Test.*—The specimen was tested to destruction under case A loading conditions, internal pressure being omitted as a safety precaution.

6. *Test Programme.*—A description of the various instruments used for initial shape and distortion measurements will be found in Reference 1. The location of the measuring sections are shown in Figs. 6, 7 and 10.

Initial Shape Measurements.—Waviness measurements were made over the chordwise sections A, B and C (Fig. 7) on upper and lower surfaces using gauge lengths of 2 in., 3 in., 4 in., 5 in. and 6 in. and section D on the upper surface. Waviness measurements in a spanwise direction were made over sections 1, 2 and 3 on the upper surface and 4, 5 and 6 on the lower surface (Fig. 7). For purposes of this report only the results of the 2 in. gauge length traverses will be considered.

Traverse gauge measurements were made on spanwise and chordwise skin joint " steps " and rivet head smoothness (Fig. 6). Short spanwise traverse gauge measurements were also made on sections 1, 2 and 3 on the upper surface.

Details of the tests made after the completion of the initial shape measurements are tabulated below.

Test	Loading Case	Maximum Factor Achieved	Loads Applied	Measurements	Remarks
Measurement of end conditions	—	—	Bending only	Horizontal approach of end bulkheads. Measured by pairs of dial gauges placed symmetrically about the neutral axis.	Maximum load applied 2,500 lb. ft.
Elastic Distortions	Gust	1	Pressure	Surface distortions on sections (1–5) panels A and B (Fig. 14). Vertical deflection of spars. Waviness over section D (Fig. 20).	Surface distortions were measured with a dial board[1].
		$1\frac{1}{4}$	Pressure and torsion		
		$1\frac{1}{4}$	Pressure and bending		
		$1\frac{1}{4}$	Pressure and bending and torsion		
Proof Tests	Case A	3 $4\frac{1}{2}$ 6 7 8 9 10	Pressure bending and torsion	Surface distortions on sections 1–5 panels A and B. Vertical deflection of the spars.	Internal air pressure was not increased with factor above $n = 6$.
	Case C	2	Pressure bending and torsion		
Ultimate	Case A	21·15 (failure)	Bending and torsion	Vertical deflection of the spars.	Air pressure omitted.

7. *Method of Test.*—7.1. *Test Rig.*—The specimen was tested in a similar way to that described in Reference 1. For the elastic distortion and proof tests this rig was modified as the loads were small. The bending load was applied by pulling the tops of the bending beams together with a turnbuckle, the load being measured by a spring balance. The torsion was applied by dead weight loading. For the ultimate test the loads were applied by the rig shown in Fig. 5.

7.2. *Tests on Spar Flange.*—It was suspected that the failure of the spars in the ultimate test was caused by torsional instability. In order to get data for estimating the torsional instability load for the flange the torsional stiffness was measured by applying a torque to a 2-ft. length of spar and measuring the twist over this length.

To provide further data on the behaviour of the spar flange under compression, strut tests were made on 12-in. and 6-in. lengths.

7.3. *Measuring Apparatus.*—The instruments used were a waviness gauge, traverse gauge and a dial board mounted on pedestal blocks glued to the wing surface over the front and rear spars. These instruments are described by King[1] (1945).

The vertical deflections of the spars were measured by 6 dial gauges mounted vertically below the spars as shown in Fig. 2.

8. *Summary of Results.*—8.1. *Initial Shape Measurements.*—The results of the waviness gauge measurements are shown in Figs. 7 and 8. The spanwise traverse gauge measurements are shown in Fig. 8 plotted above the waviness gauge results.

The traverse gauge measurements of the skin joint " step " and rivet head smoothness are shown in Fig. 6. The critical values for the rivet head smoothness and skin joint " step " are also shown in this figure.

The waviness gauge results given are the dial gauge readings plotted against the position of the centre of the gauge on the wing surface. No attempt has been made to obtain the curvature of the wing from the gauge readings. The method adopted for analysing[3] the results was to draw an envelope to the waviness gauge graph for a 2-in. gauge length and to measure the width of this band. Using as the critical value of wave size on the wing surface one having a ratio of height to length of $\frac{1}{1000}$ in a chordwise direction and $\frac{3}{1000}$ in a spanwise direction, then the maximum permissible width of the envelope to the curvature gauge graph is 0·004 in. for chordwise traverses and 0·012 in. for spanwise traverses. Fig. 9 shows the position on the traverses at which the width of envelope exceeded the permissible values.

8.2. *Elastic Distortion Tests.*—Graphs of the wing surface distortion plotted against the chord for the measuring sections B1–5 are shown in Figs. 11–13. Since measurements taken on panel A were in close agreement with those taken on panel B only the latter are shown. For each measuring section graphs are drawn showing the distortions due to pressure alone at $n = 1$ and to pressure, bending and torsion at $n = 1$ and $1\frac{1}{4}$. The magnitude of the distortions on measuring sections over a rib, a stiffener and midway between a rib and stiffener, and tabulated in Fig. 14. For each section the dimensions of the following three waves are given :—The convex wave forward of the front spar, the concave wave over the front spar and the convex wave between the two spars. From the graphs it will be seen that the maximum distortions forward and aft of the front spar occur at 13 per cent. and 40 per cent. chord respectively. Accordingly the deflection of the skin along a spanwise line has been deduced for these points and is shown in Fig. 13. Load deflection curves for the skin at the 13 per cent. and 40 per cent. chord positions are shown in Fig. 13.

The results of a 2-in. waviness gauge traverse over the wing at section D when subjected to pressure at $n = 1$ and combined pressure, bending and torsion at $n = 1$, together with the initial shape measurements of this section are shown in Fig. 16. These measurements were made to ascertain the effect of these loads on the initial waviness of the skin.

The central bending deflection of the spars and twisting of the specimen over the test length plotted against load are shown in Fig. 17.

8.3. *Proof Tests.*—Tests were made under case A loading conditions up to a maximum factor of $n = 10$. The bending torsion and pressure were increased with factor up to $n = 6$ above this load bending and torsion were increased with factor, pressure being maintained at its $6g$ value. The internal pressure was kept constant at factors above $6g$ as it is a function of the speed and not the stress conditions in the structure.

Chordwise plots of the skin distortion for positions B1, B3 and B5 at factors of $n = 2$, 6 and 10 are shown in Fig. 16, together with spanwise plots of skin distortion for the 13 per cent. and 40 per cent. chord positions and load deflection graphs for the same two points. The bending deflection of the centre point of the spars over the test length and twisting of the specimen are also shown in the same figure.

Since no permanent distortion of the specimen was observed in these tests, it was decided to test the specimen under aileron case C (maximum torque) loading conditions. No permanent distortion was observed, after the specimen had been loaded up to a factor of $n = 2$, which was the ultimate design factor for this case.

The chordwise distortions of the skin together with the load deflection graphs and spanwise distortion of the skin at the 13 per cent. and 40 per cent. chord positions are shown in Fig. 2. The bending deflection of the spars and twisting of the test length are shown in the same figure.

8.4. *Ultimate Test.*—Fig. 18 shows twisting and bending deflections of the spars over the test length up to a factor of $n = 17$. The vertical dials were removed at this load as failure of the specimen might have damaged the gauges.

As the load factor was increased buckling of the top skin was noticed on one or two panels at $n = 3$. At $n = 5$ all inter-spar panels were slightly buckled, but no buckling forward of the front spar was observed until a factor of $n = 11$ was reached. At $n = 13$ inter-rivet buckling of the skin over the front spar occurred and at $n = 19$ inter-rivet buckling over the rear spar was observed. No damage to the under-surface apart from appreciable opening of the chordwise skin joints was observed. Failure occurred at a factor of $n = 21 \cdot 15g$. A photograph of the failure is shown in Fig. 19.

8.5. *Strut Tests on Spar Flange.*—The 12-in. and 6-in. lengths of flange failed at 48,800 lb./sq. in. and 59,500 lb./sq. in. respectively. The torsional stiffness of the flange was found to be 8,800 lb./in. per inch length.

REFERENCES

No.	*Author*	*Title, etc.*
1	J. C. King	An Experimental Investigation into the suitability of a Corrugated Construction Wing for a Laminar Flow Aerofoil. R.A.E. Report No. S.M.E. 3291. A.R.C. 8852. January, 1945. (To be published.)
2	E. J. Richards, W. S. Walker and B. Thwaites.	Drag Tests on Samples of Laminar Flow Aerofoil. (3) Short Bros. A.R.C. 8392. February, 1945. (Unpublished.)
3	J. C. King and D. H. Trollope	A Method of Testing Smooth Wings for Initial Shape and Resistance to Distortion under Load. R.A.E. Report No. S.M.E. 3327. A.R.C. 8816. May, 1945. (To be published.)

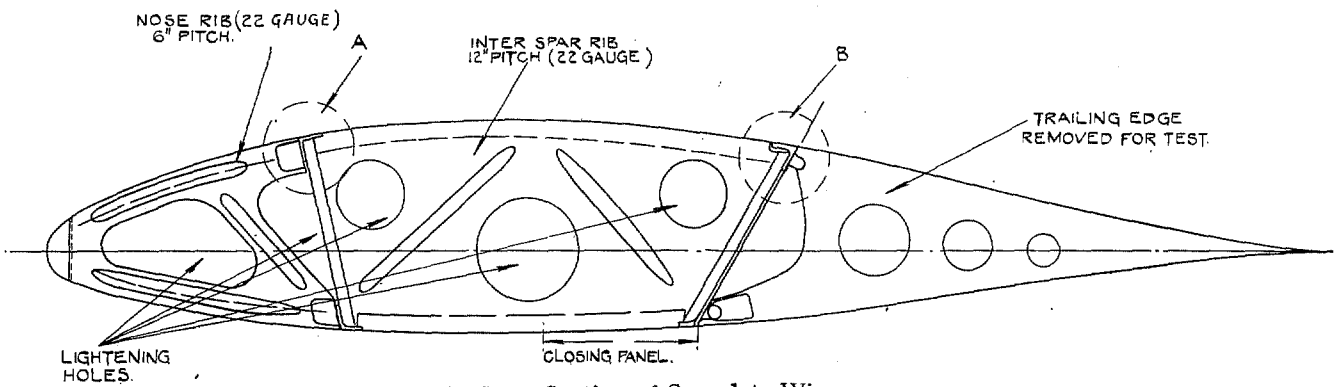

Cross Section of Complete Wing

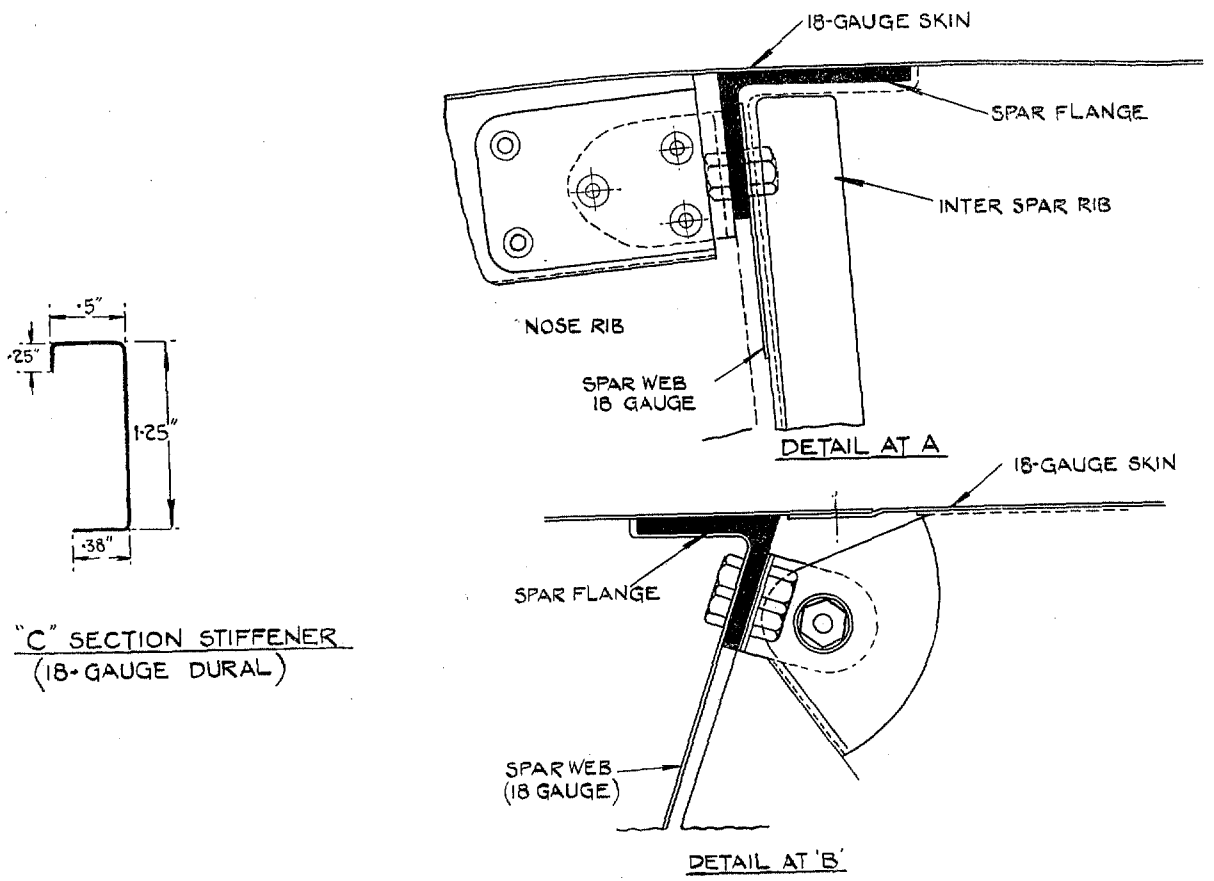

FIG. 1. Details of Wing Construction.

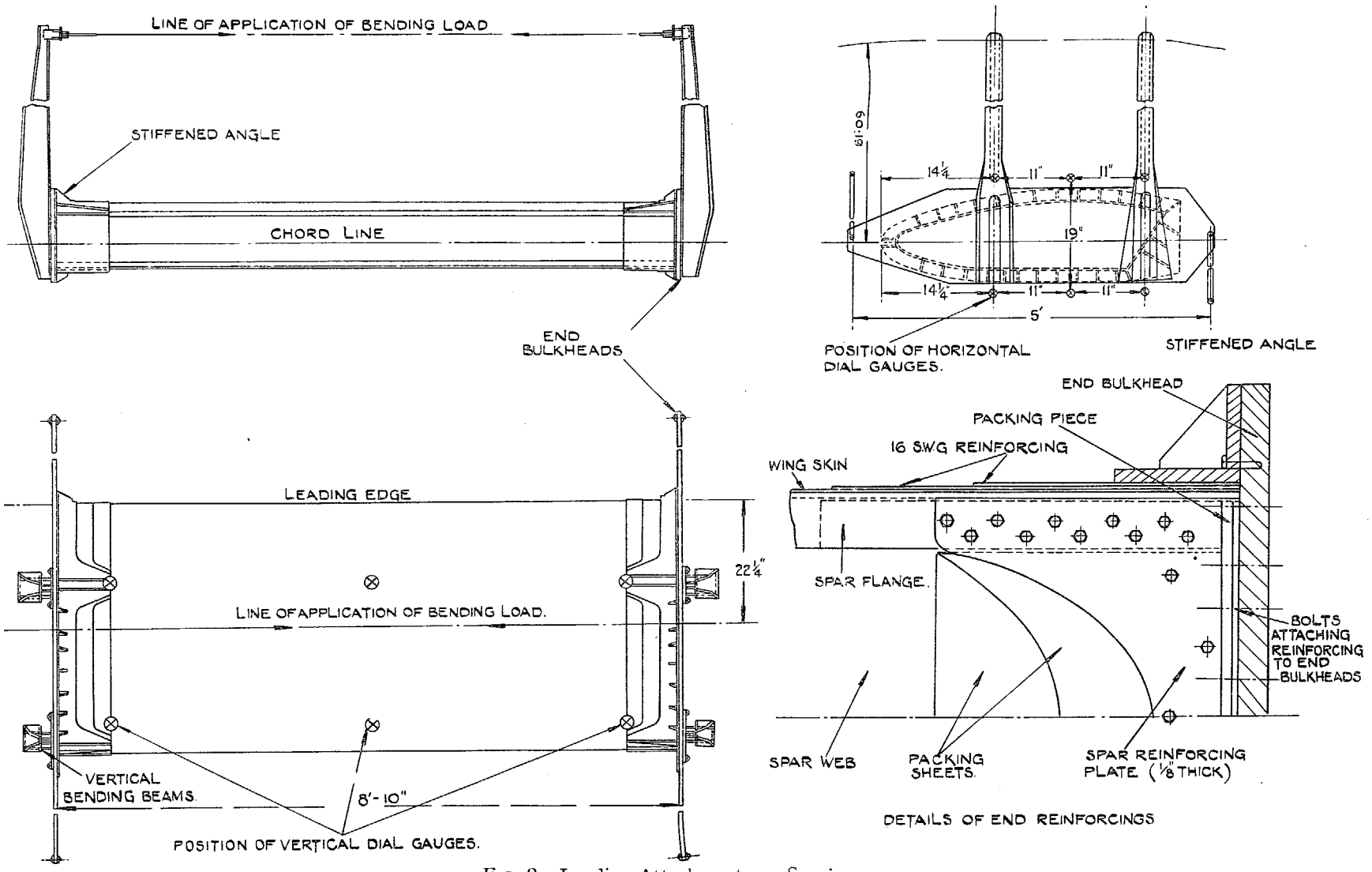

FIG. 2. Loading Attachments on Specimen.

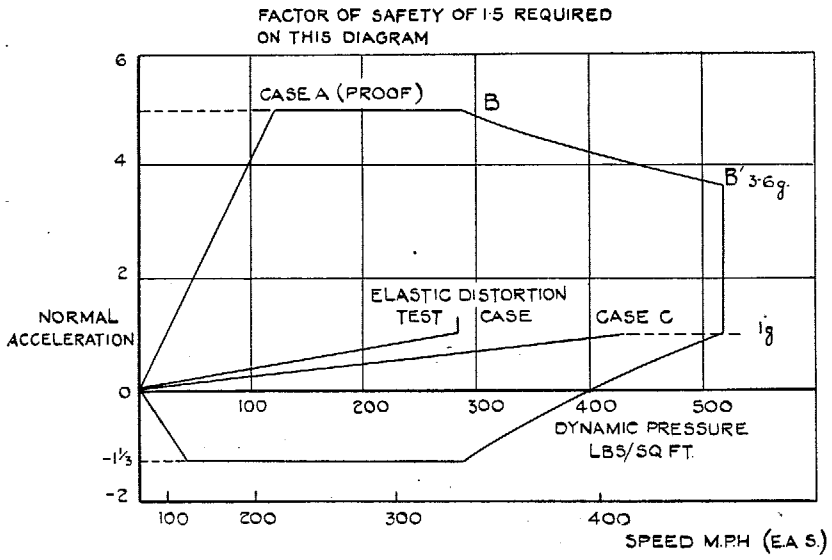

Test Loads at Factor $n=1g$

Case	Test	Bending Moment	Torsion	Internal Pressure
Max. Speed Level Flight	Elastic Distortion	13,320 lb. in.	12,180 in. lb.	187·2 lb./sq. ft.
Case C Ailerons Max. Torque	Proof	3,750 lb. in.	40,350 in. lb.	144 lb./sq. ft.
Case A	Proof and Ultimate	9,540 lb. in.	1,320 in. lb.	36·6 lb./sq. ft.

FIG. 3. Rationalised Stressing Diagram Showing Test Cases.

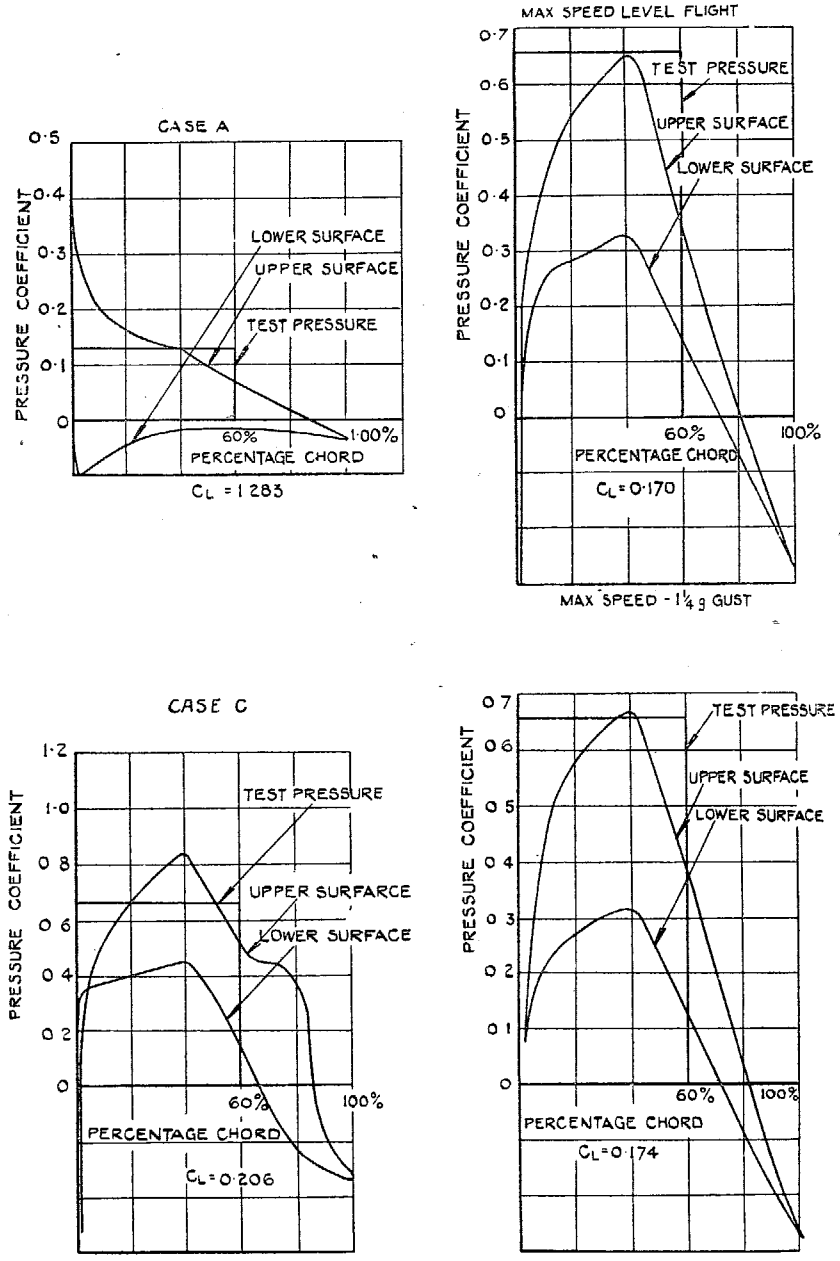

FIG. 4. Pressure Distribution Diagrams.

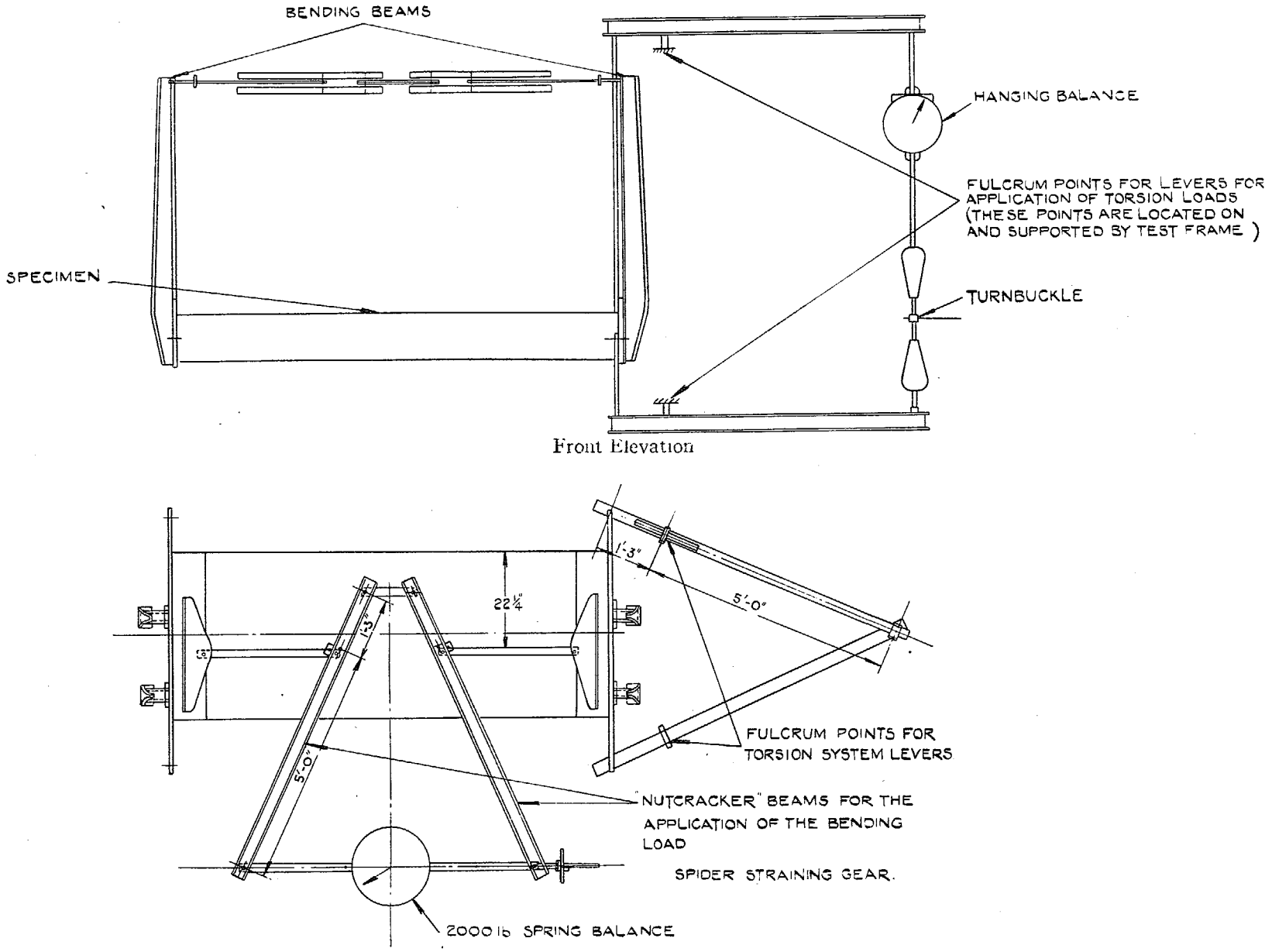

FIG. 5. Loading Rig for Ultimate Test.

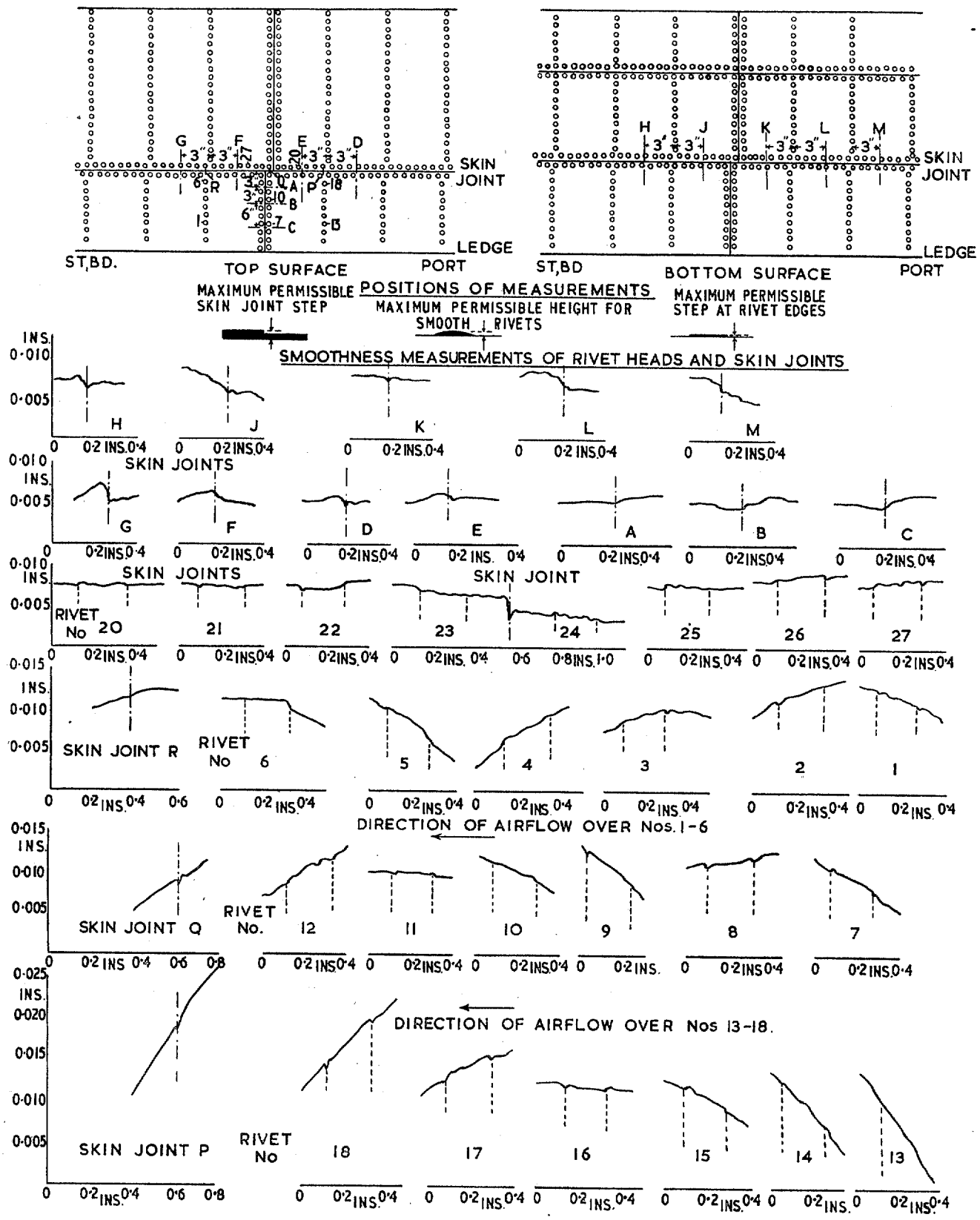

FIG. 6. Smoothness Measurements of Rivet Heads and Skin Joints.

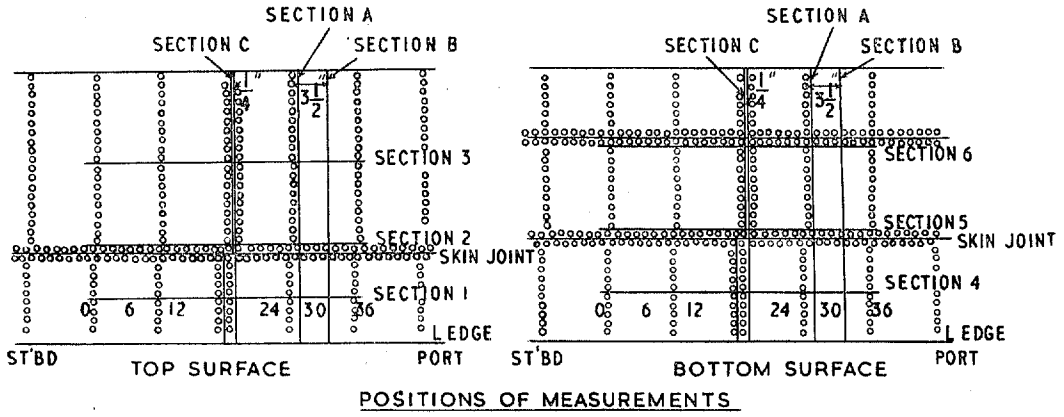

POSITIONS OF MEASUREMENTS

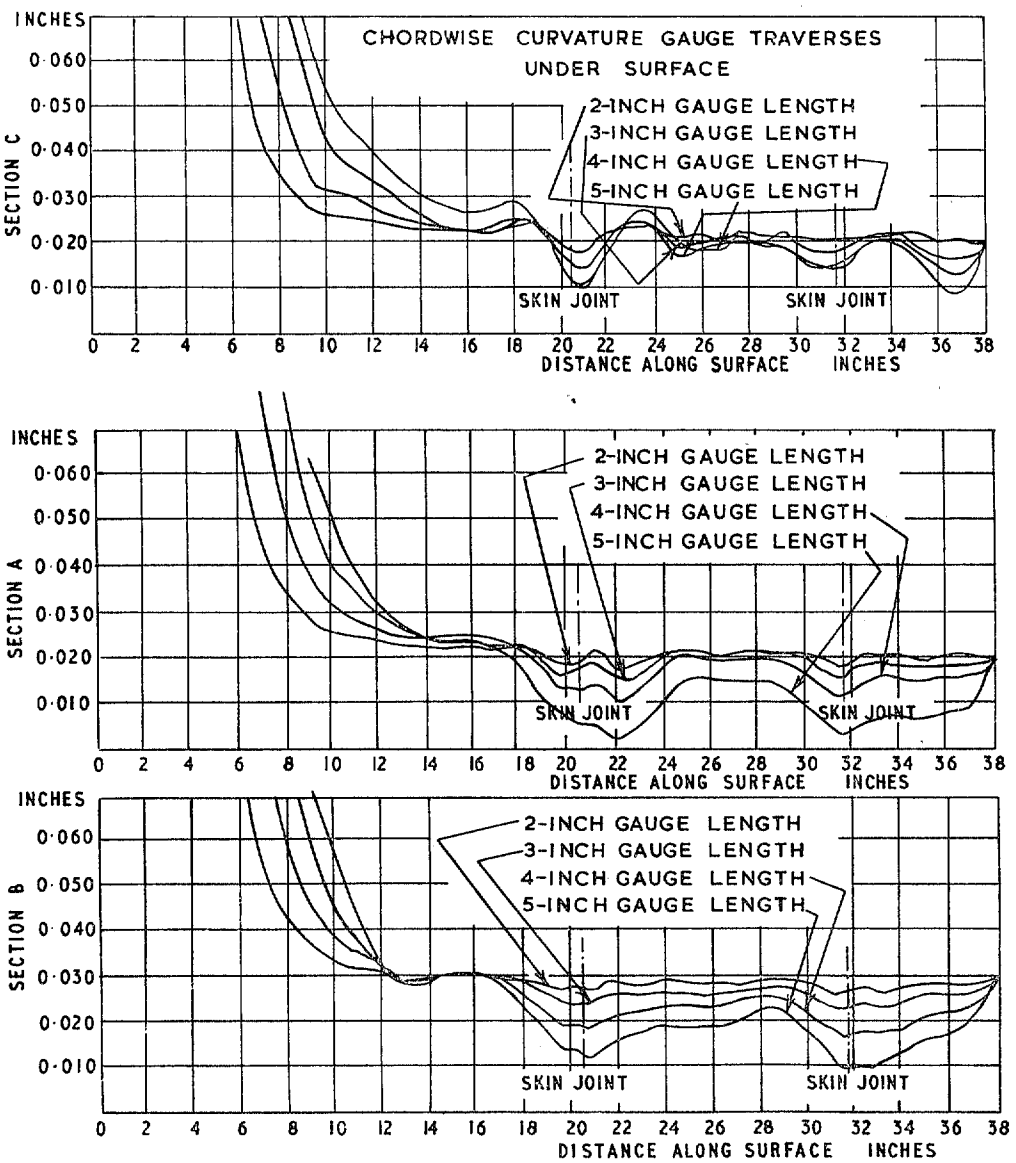

FIG. 7. Chordwise Waviness Measurements.

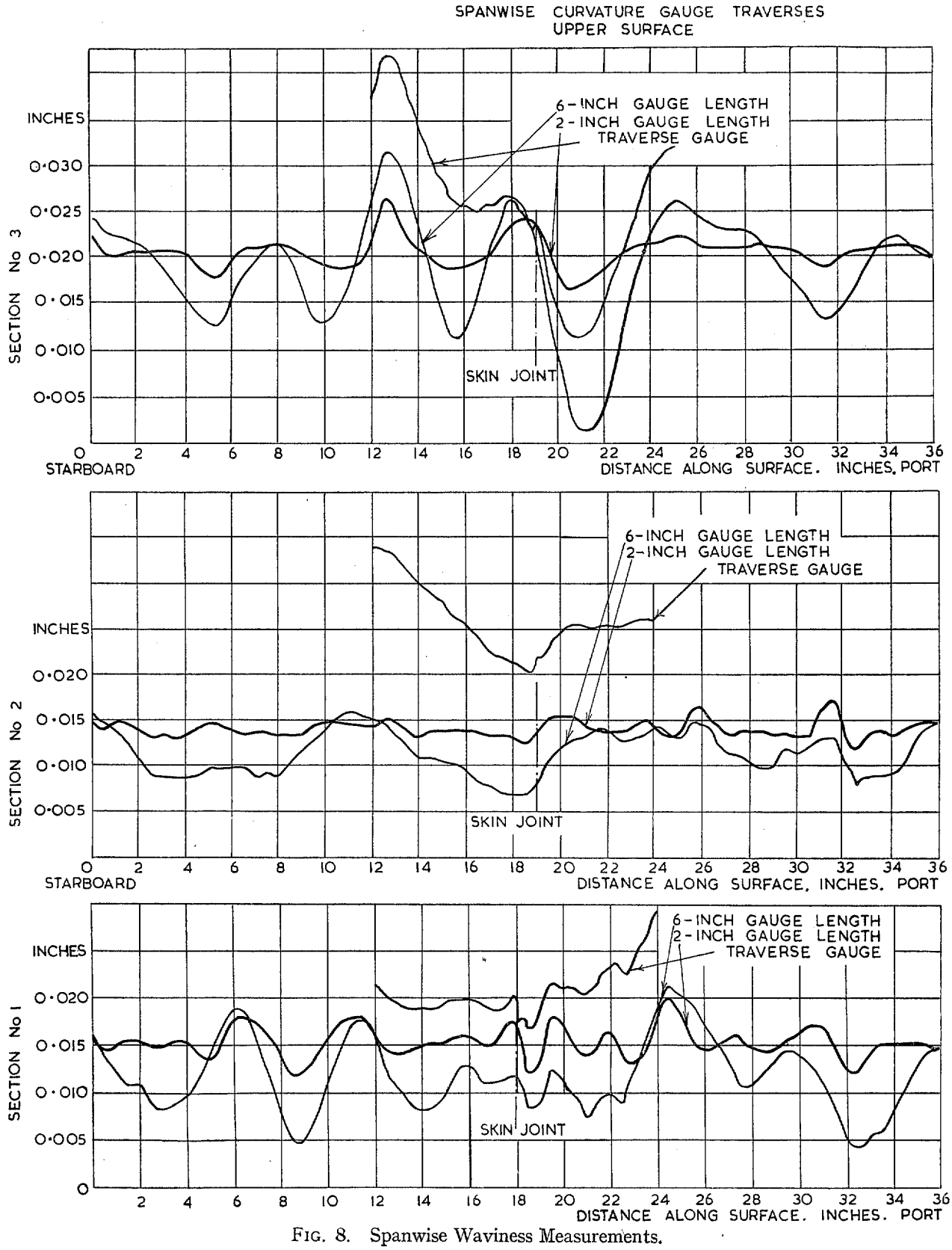

FIG. 8. Spanwise Waviness Measurements.

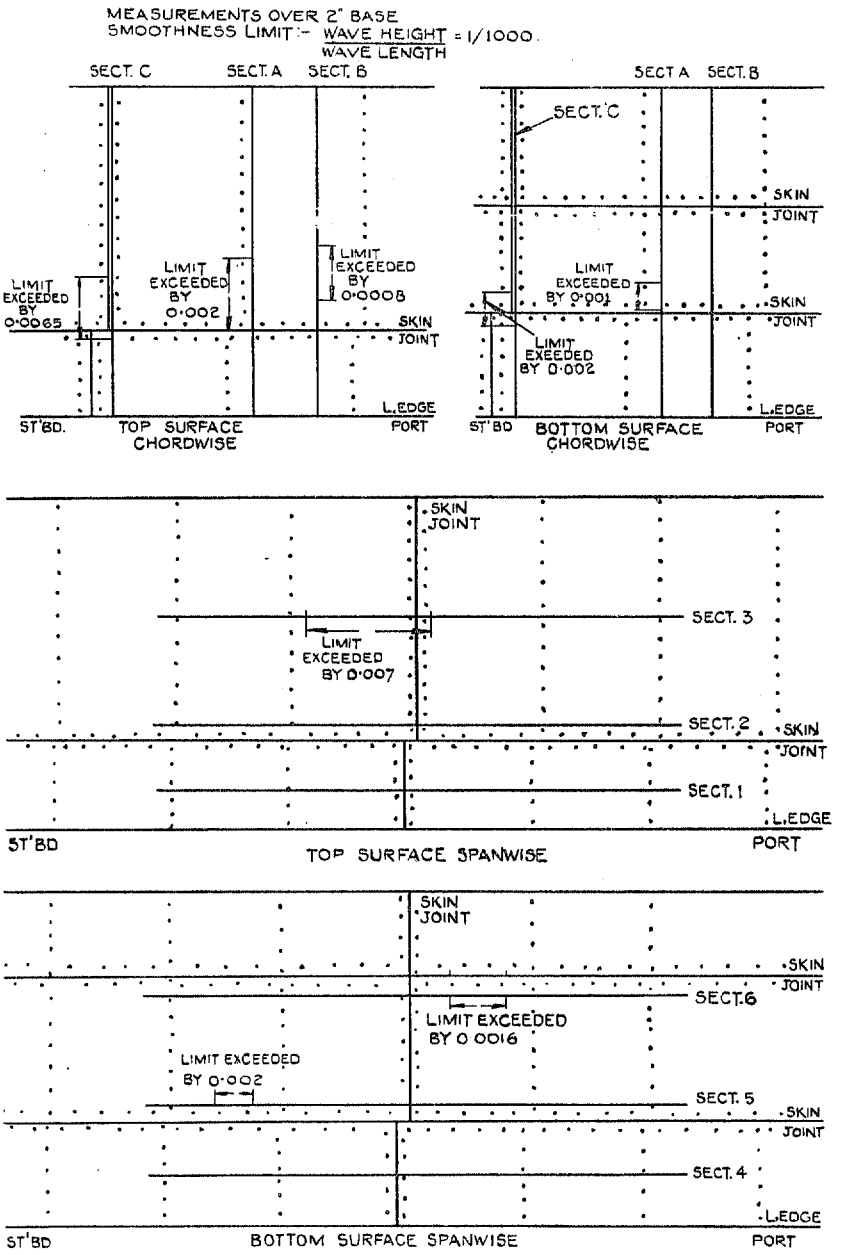

FIG. 9. Locations of Excessive Skin Waviness.

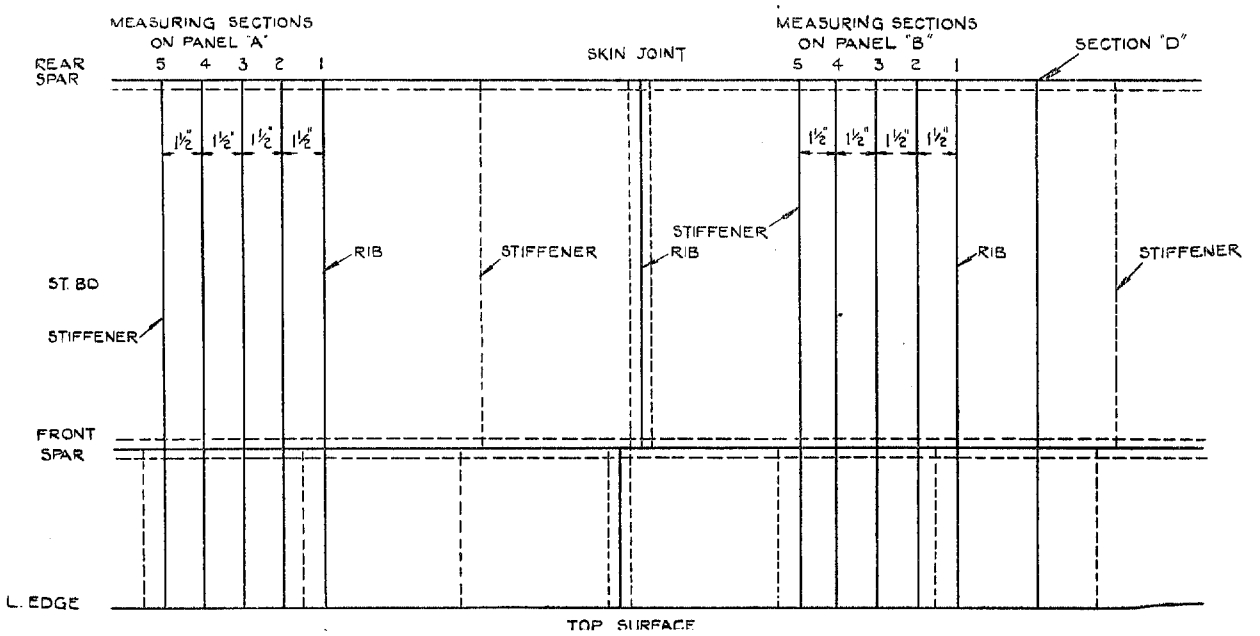

FIG. 10. Positions of Measuring Sections.

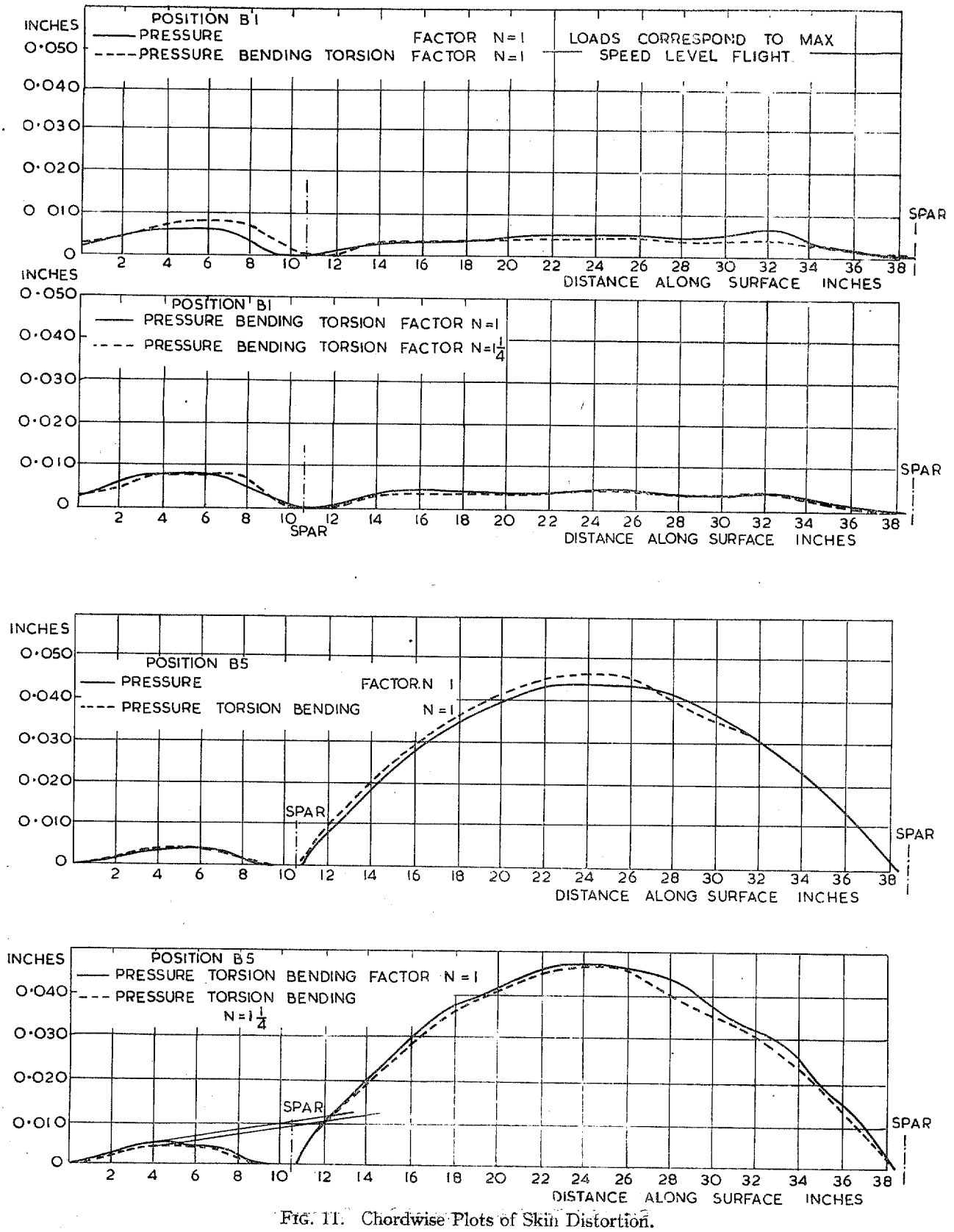

FIG. 11. Chordwise Plots of Skin Distortion.

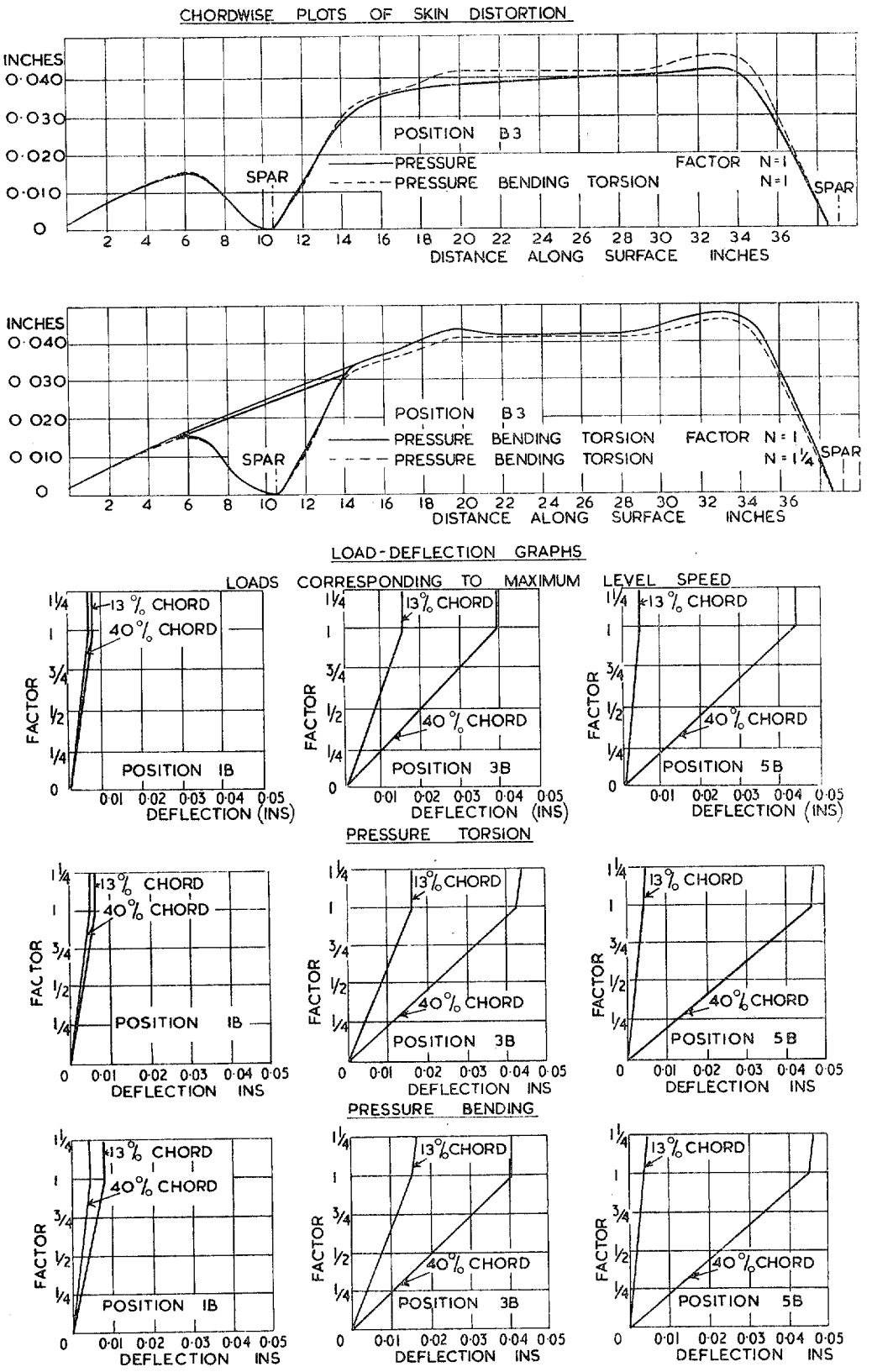

FIG. 12. Chordwise Plots of Skin Distortion.

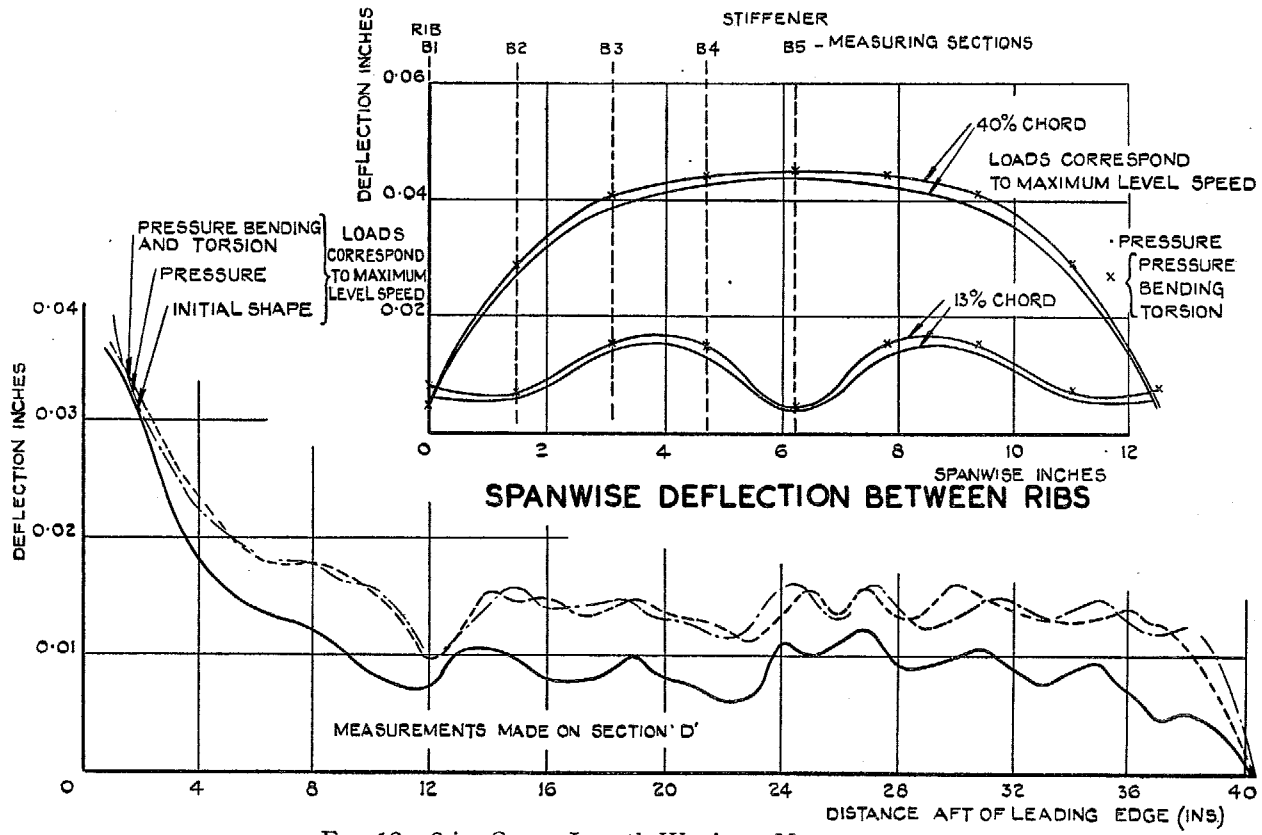

FIG. 13. 2-in. Gauge Length Waviness Measurements.

Position of Wave		Position on Graphs (ins.)	Ratio $\frac{\text{Wave Height}}{\text{Wave Length}}$	Ideal Ratio	Loading Conditions
	L. Edge	0–9	0·0007	0·001	Pressure $N = 1$
	Over Spar	6–14	0·0006	0·001	
	Inter-Spar	11–39	0·0002	0·001	
	L. Edge	0–10½	0·0008	0·001	Pressure Bending and Torsion $N = 1$
B_1	Over Spar	7–15	0·0008	0·001	
	Inter-Spar	11½–39	0·0002	0·001	
	L. Edge	0–10½	0·0007	0·001	Pressure Bending and Torsion $N = 1\frac{1}{4}$
	Over Spar	6–15	0·0007	0·001	
	Inter-Spar	10½–39	0·0001	0·001	
	L. Edge	0–9	0·0005	0·001	Pressure $N = 1$
	Over Spar	5½–12	0·0001	0·001	
	Inter-Spar	10½–39	0·0016	0·001	
	L. Edge	0–9	0·0004	0·001	Pressure Bending and Torsion $N = 1$
B_5	Over Spar	5–12	0·0001	0·001	
	Inter-Spar	10½–39	0·0016	0·001	
	L. Edge	0–9	0·0006	0·001	Pressure Bending and Torsion $N = 1\frac{1}{4}$
	Over Spar	4–12	0·0013	0·001	
	Inter-Spar	10½–39	0·0017	0·001	
	L. Edge	0–10½	0·0014	0·001	Pressure $N = 1$
	Over Spar	5½–15	0·0025	0·001	
	Inter-Spar	10½–39	0·0015	0·001	
	L. Edge	0–10½	0·0015	0·001	Pressure Bending and Torsion $N = 1$
B_3	Over Spar	6–15	0·0027	0·001	
	Inter-Spar	10½–39	0·0016	0·001	
	L. Edge	0–10½	0·0015	0·001	Pressure Bending and Torsion $N = 1\frac{1}{4}$
	Over Spar	5½–15	0·0027	0·001	
	Inter-Spar	10½–39	0·0017	0·001	

FIG. 14. Magnitude of Skin Distortions.

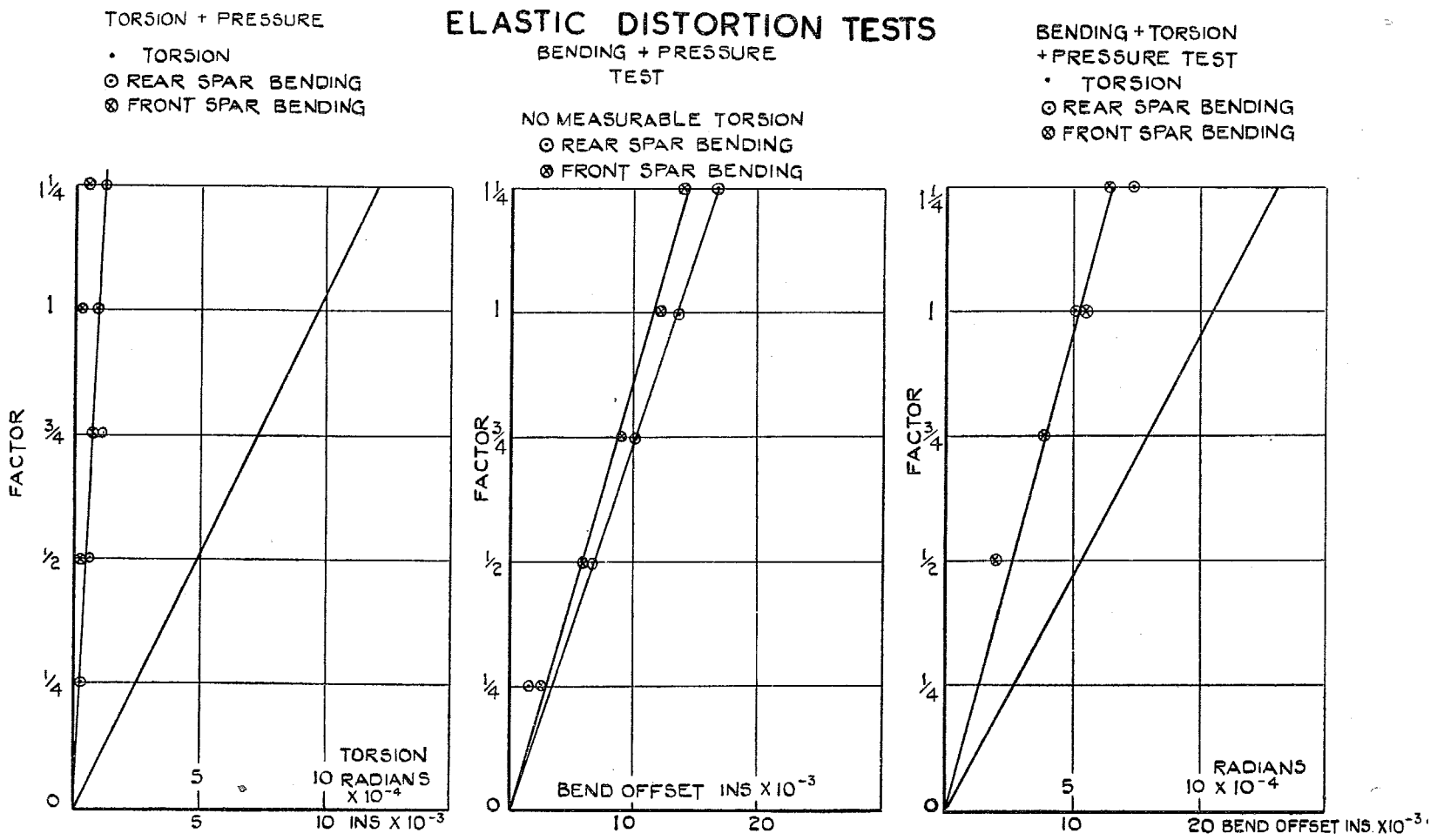

FIG. 15. Mid-point Deflections of Spars and Torsional Deflection of Specimen.

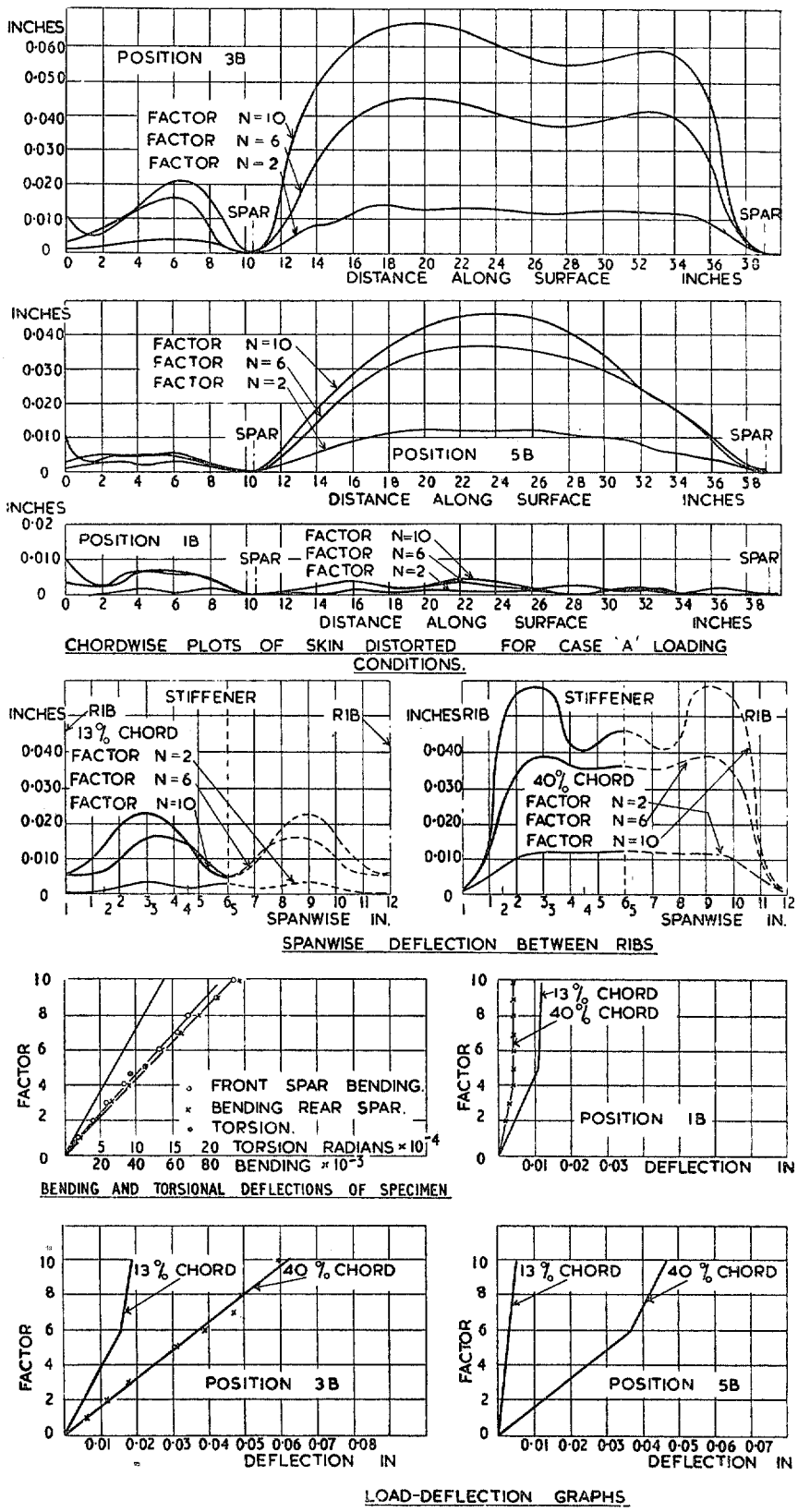
INCHES
POSITION 3B
FACTOR N=10
FACTOR N=6
FACTOR N=2
SPAR
SPAR
DISTANCE ALONG SURFACE
INCHES
POSITION 5B
POSITION 1B
CHORDWISE PLOTS OF SKIN DISTORTED FOR CASE 'A' LOADING CONDITIONS.
STIFFENER
RIB
13% CHORD
40% CHORD
SPANWISE IN.
SPANWISE DEFLECTION BETWEEN RIBS
FACTOR
FRONT SPAR BENDING.
BENDING REAR SPAR.
TORSION.
TORSION RADIANS × 10⁻⁴
BENDING × 10⁻³
DEFLECTION IN
BENDING AND TORSIONAL DEFLECTIONS OF SPECIMEN
LOAD-DEFLECTION GRAPHS

FIG. 16.

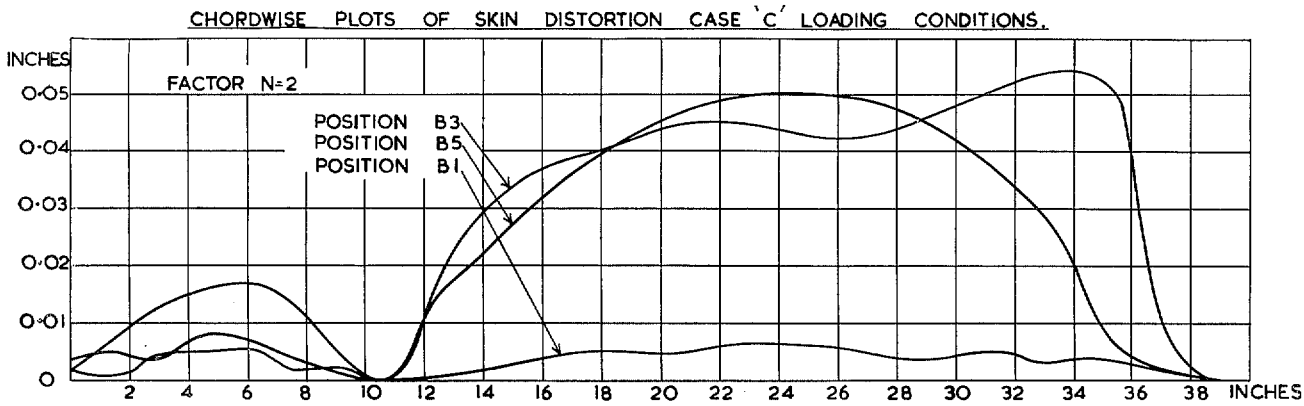

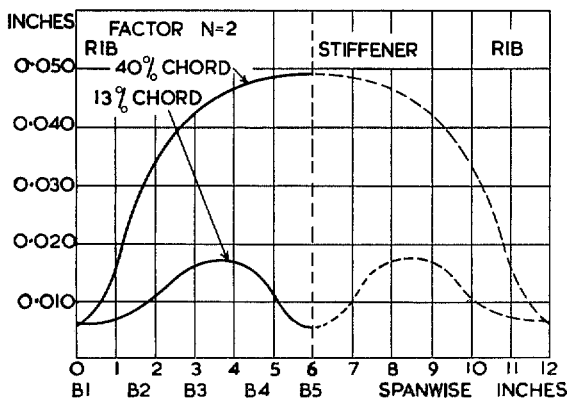

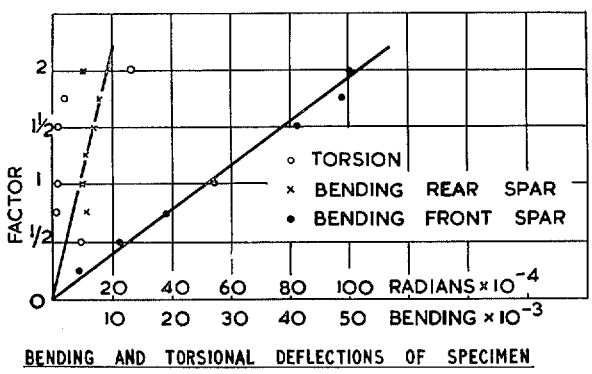

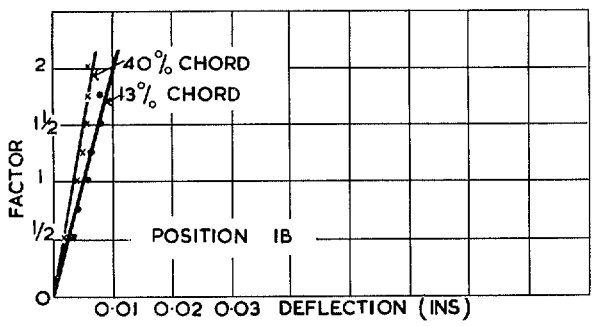

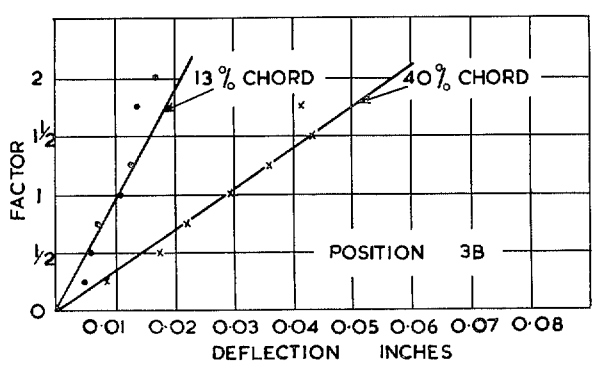

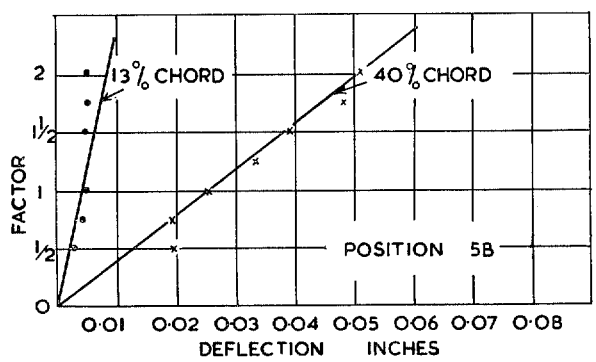

FIG. 17. Load-Deflection Graphs.

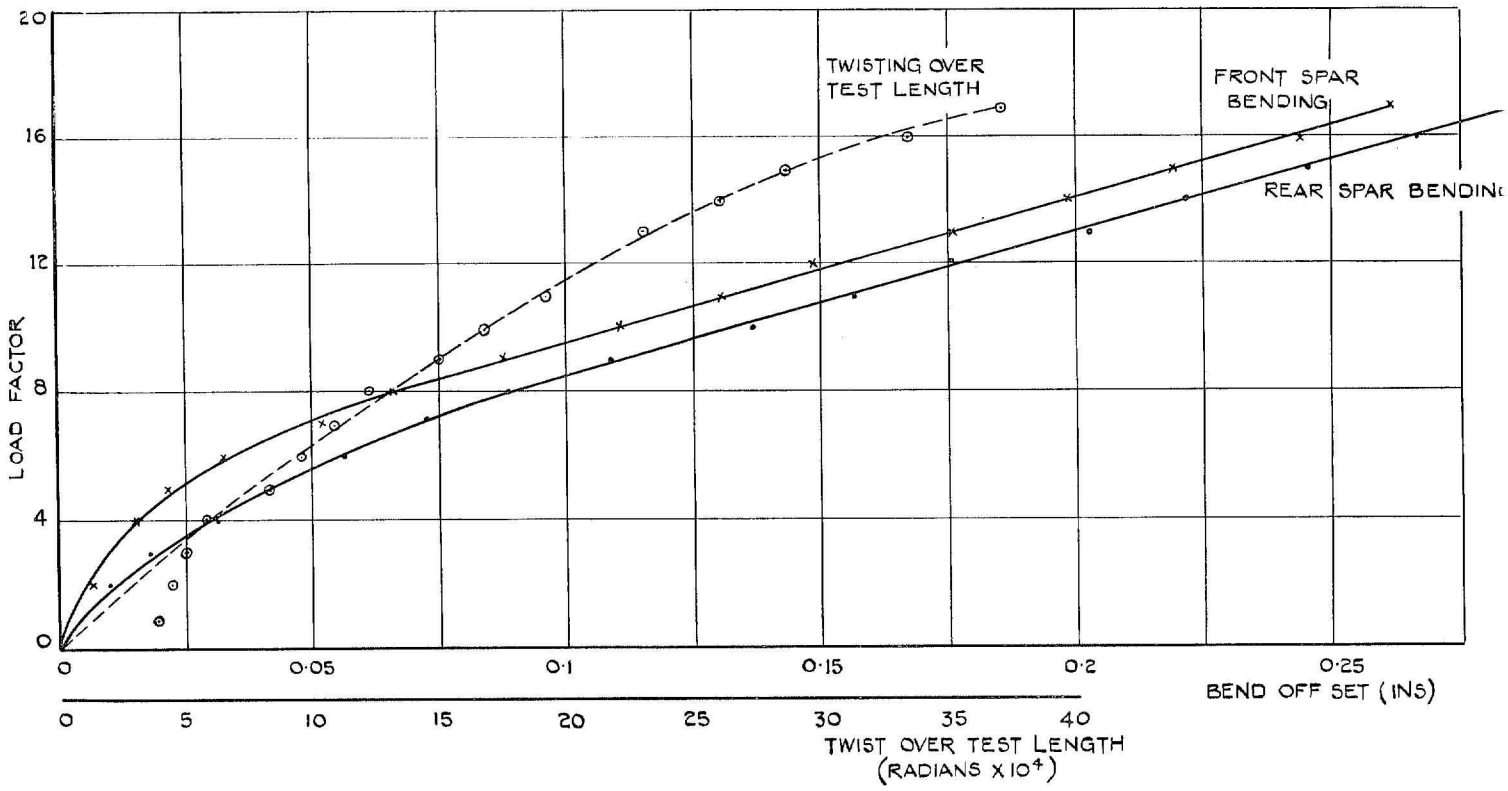

FIG. 18. Spar Deflection—Ultimate Test.

Upper front spar flange failure (view looking forward).

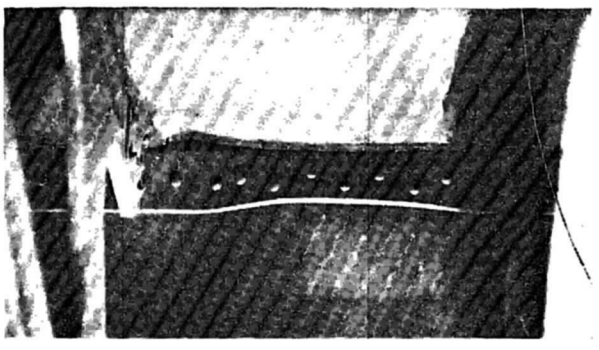

Upper front spar failure (view looking aft).

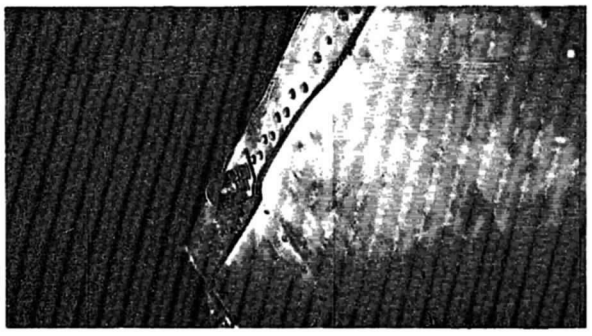

Rear spar failure.

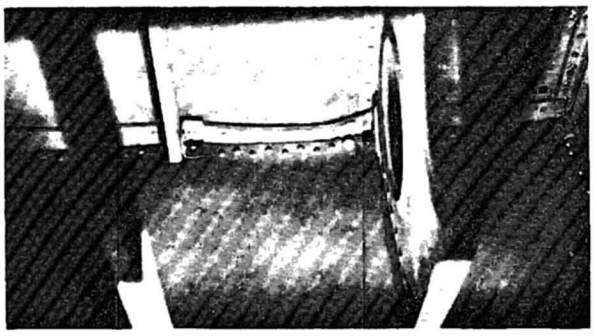

Rear spar failure.

FIG. 19.

(86252) Wt. 12/818 1/49 Hw.

PRINTED IN GREAT BR

Publications of the Aeronautical Research Committee

TECHNICAL REPORTS OF THE AERONAUTICAL RESEARCH COMMITTEE—

1934-35 Vol. I. Aerodynamics. 40*s.* (40*s.* 8*d.*)
Vol. II. Seaplanes, Structures, Engines, Materials, etc. 40*s.* (40*s.* 8*d.*)

1935-36 Vol. I. Aerodynamics. 30*s.* (30*s.* 7*d.*)
Vol. II. Structures, Flutter, Engines, Seaplanes, etc. 30*s.* (30*s.* 7*d.*)

1936 Vol. I. Aerodynamics General, Performance, Airscrews, Flutter and Spinning. 40*s.* (40*s.* 9*d.*)
Vol. II. Stability and Control, Structures, Seaplanes, Engines, etc. 50*s.* (50*s.* 10*d.*)

1937 Vol. I. Aerodynamics General, Performance, Airscrews, Flutter and Spinning. 40*s.* (40*s.* 9*d.*)
Vol. II. Stability and Control, Structures, Seaplanes, Engines, etc. 60*s.* (61*s.*)

1938 Vol. I. Aerodynamics General, Performance, Airscrews, 50*s.* (51*s.*)
Vol. II. Stability and Control, Flutter, Structures, Seaplanes, Wind Tunnels, Materials. 30*s.* (30*s.* 9*d.*)

ANNUAL REPORTS OF THE AERONAUTICAL RESEARCH COMMITTEE—

1933-34 1*s.* 6*d.* (1*s.* 8*d.*)
1934-35 1*s.* 6*d.* (1*s.* 8*d.*)
April 1, 1935 to December 31, 1936. 4*s.* (4*s.* 4*d.*)
1937 2*s.* (2*s.* 2*d.*)
1938 1*s.* 6*d.* (1*s.* 8*d.*)

INDEXES TO THE TECHNICAL REPORTS OF THE ADVISORY COMMITTEE ON AERONAUTICS—

December 1, 1936 — June 30, 1939.	R. & M. No. 1850.	1*s.* 3*d.* (1*s.* 5*d.*)
July 1, 1939 — June 30, 1945.	R. & M. No. 1950.	1*s.* (1*s.* 2*d.*)
July 1, 1945 — June 30, 1946.	R. & M. No. 2050.	1*s.* (1*s.* 1*d.*)
July 1, 1946 — December 31, 1946.	R. & M. No. 2150.	1*s.* 3*d.* (1*s.* 4*d.*)
January 1, 1947 — June 30, 1947.	R. & M. No. 2250.	1*s.* 3*d.* (1*s.* 4*d.*)

Prices in brackets include postage.

Obtainable from

His Majesty's Stationery Office

London W.C.2 : York House, Kingsway
[Post Orders—P.O. Box No. 569, London, S.E.1.]
Edinburgh 2 : 13A Castle Street
Birmingham 3 : 2 Edmund Street
Bristol 1 : Tower Lane
Manchester 2 : 39 King Street
Cardiff : 1 St. Andrew's Crescent
Belfast : 80 Chichester Street
or through any bookseller.